MRS Communications (2018), *8*, 1135–1138
© Materials Research Society, 2018
doi:10.1557/mrc.2018.165

MRS Communications

Research Letter

Supercapacitor electrodes with high active mass loading

R. Poon and **I. Zhitomirsky,** Department of Materials Science and Engineering, McMaster University, Hamilton, Ontario, L8S4L7, Canada
Address all correspondence to I. Zhitomirsky at E-mail: **zhitom@mcmaster.ca**

(Received 25 April 2018; accepted 6 August 2018)

Abstract

We report the fabrication and testing of MnO_2–carbon nanotube (NT) electrodes for supercapacitors (SCap) with high active mass (AM). Cetylpyridinium chloride surfactant was used as a capping agent for synthesis and a phase transfer agent for the liquid–liquid extraction. Water immiscible solvent, *n*-butanol, was used as a receiving and reducing medium for the synthesis of MnO_2 from cetylpyridinium permanganate. Improved co-dispersion and nanoscale mixing of MnO_2 and NT enabled the fabrication of advanced electrodes with mass loading of 42–61 mg/cm^2, ratio of AM to current collector mass of 0.63–0.91, which showed the highest capacitance of 8.95 F/cm^2.

Introduction

MnO_2 has gained significant interest as a supercapacitor (SCap) material due to its high gravimetric capacitance (C_g, F/g), large and stable voltage window in Na_2SO_4 aqueous electrolyte, low toxicity, and low cost.[1–6] The charging process is described by the below equation:

$$MnO_2 + R^+ + e^- \leftrightarrow MnO_2R \quad (1)$$

Small size of MnO_2 particles and porous electrode microstructure enable good ion access ($R^+ = H^+$, Na^+, and K^+) to the particle surface.[7] Carbon nanotube (NT) additives allow for improved electronic conductivity of MnO_2–NT composites.[8–10] Despite the impressive progress[4,8,11–14] achieved in the design of MnO_2-based composites, there is a need for the manufacturing of advanced SCap electrodes with high active mass (AM) for practical applications. It is known that C_g decreases significantly with increasing AM.[15] Moreover,[15] limited electrolyte access to AM can result in reduction of areal capacitance (C_S, F/cm^2) with increasing AM. In this scenario, the bulk material exhibits low capacitance whereas surface region is highly capacitive, and the overall capacitance is reduced since total capacitance is governed by the capacitor with lower capacitance. A high C_S must be achieved at low electrode resistance. Another important characteristic of the SCap electrodes is the ratio (δ_m) of AM to current collector mass. It should be noted that δ_m values are often about 0.5–2% for films with AM of 0.5–1.0 mg/cm^2 on metal foils. Substantially higher δ_m values are required for advanced lightweight SCap.

The objective of this study was the development of MnO_2–NT electrodes with high AM and enhanced performance. Our conceptually novel manufacturing method is based on the synthesis of surfactant–MnO_4 complex compound for the MnO_2 fabrication. The surfactant inhibited MnO_2 particle growth, enabled liquid–liquid extraction of MnO_2, and formation of composites with improved morphology. This method eliminated the problems related to the MnO_2 particle agglomeration during filtration and drying and their re-dispersion in the electrode processing medium. Moreover, the method facilitated improved co-dispersion and nanoscale mixing of non-agglomerated MnO_2 and NT, which enabled enhanced performance of the composite electrodes at high AM. We fabricated electrodes with AM of 42–61 mg/cm^2 and δ_m values of 0.63–0.91. The C_S of 8.95 F/cm^2 was achieved.

Experimental procedures

Commercial cetylpyridinium chloride (CPC), $KMnO_4$, Na_2SO_4, poly(vinyl butyral) (PVB), *n*-butanol, multiwalled NTs (ID of 4 nm, OD of 13 nm, length in the range of 1–2 μm, Bayer Company, Germany), and Ni foam (porosity of 95%, Vale, Canada) were used.

Solutions of 3.45 mM CPC in 150 mL of deionized (DI) water and 3.45 mM $KMnO_4$ in 50 mL of DI water were prepared and stirred for 15 min. Mixing of the solutions resulted in the synthesis of cetylpyridinium permanganate precipitate. The addition of 50 mL of *n*-butanol as a reducing agent and stirring for 1 h allowed for the synthesis of MnO_2 particles. The particles were spontaneously transferred to the *n*-butanol phase, whereas the aqueous phase became clear. The suspension of MnO_2 particles was filtered, then washed and dried particles were studied by x-ray diffraction (XRD). The results of XRD studies presented below confirmed the formation of MnO_2. The drying of the particles resulted in their agglomeration.

NT were added to water and ultrasonicated. It was found that the addition of *n*-butanol resulted in the transfer of NT to the

https://doi.org/10.1557/mrc.2018.165 Published online by Cambridge University Press

n-butanol phase, whereas the aqueous phase became clear (Supplementary Fig. S1). This observation paved the way for the phase transfer of the as-prepared MnO_2 and NT from water to the *n*-butanol phase. Therefore, the procedure for the synthesis of MnO_2 was modified by adding NT to the synthesis medium. In the modified procedure, NTs were dispersed in water in the presence of CPC surfactant, which facilitated NT dispersion. Then, $KMnO_4$ solution was added to form cetylpyridinium permanganate. The addition of *n*-butanol to the mixture, containing cetylpyridinium permanganate and NTs, resulted in the MnO_2 synthesis and co-dispersion of MnO_2 and NT in the *n*-butanol phase (Supplementary Fig. S2). The mass ratio of MnO_2 and NT was 4:1. The slurry, containing MnO_2 and NT in a solvent, containing dissolved PVB binder, was used for the impregnation of Ni foam current collectors. The AM loading of MnO_2 and NT of the electrodes was in the range of 42–61 mg/cm^2. The mass of the PVB binder was in the range of 0.5–1% of the total AM. The electrodes were dried at 60 °C for 48 h.

XRD analysis was performed using a powder diffractometer equipped with a Bruker SMART6000 CCD area detector and a Rigaku Cu K_α rotating anode. Scanning electron microscopy (SEM) and electrochemical characterization methods were described in Ref. 15.

Results and discussion

Previous investigations showed that interactions of cationic surfactants and other long chain organic cations with permanganates resulted in the formation of complex compounds, such as cetyltrimethylammonium permanganate,[16] triphenylphosphonium permanganate,[17] tetrabutylammonium permanganate,[18] and other compounds,[19,20] which were used as oxidants for many applications.[19] In this investigation, we prepared cetylpyridinium permanganate by reaction of CPC and $KMnO_4$ in water. The addition of *n*-butanol allowed synthesis of MnO_2 in the *n*-butanol phase. The synthesis of MnO_2 was confirmed by the XRD analysis (Fig. 1). The XRD pattern showed reflections of the birnessite phase. However, the mechanism of MnO_2 formation is not well understood. Previous investigations[21] showed that the reduction of Mn^{7+} species at the interface of aqueous $KMnO_4$ solutions and *n*-butanol resulted in the precipitation of MnO_2 in water. In contrast, in this investigation we prepared cetylpyridinium permanganate in water and the addition of *n*-butanol led to the formation of MnO_2 in the *n*-butanol phase. The analysis of the literature indicated that cationic surfactants facilitate[22] phase transfer of MnO_4^- species from water to an organic phase. The organic phase, containing transferred MnO_4^- species has been separated and the addition of a reducing agent to the organic phase allowed the fabrication of MnO_2 particles.[22]

We suggested that stirring of the mixture, containing cetylpyridinium permanganate and *n*-butanol, resulted in the phase transfer of cetylpyridinium permanganate from water to *n*-butanol and its dissociation in the *n*-butanol phase. The redox reaction of MnO_4^- species with *n*-butanol resulted in the precipitation of MnO_2, which remained in the *n*-butanol phase. We suggested that surfactant was adsorbed on the MnO_2 particles during synthesis and surfactant modified particles were dispersed in *n*-butanol. In the previous studies performed without surfactant,[21] the MnO_2 prepared by the reduction of MnO_4^- species with *n*-butanol, precipitated in an aqueous phase.

The ability to synthesize and disperse MnO_2 particles in the organic phase offers benefits for SCap applications. In previous investigations,[23] MnO_2 particles were synthesized from aqueous $KMnO_4$ solutions, then dried and dispersed again in an organic phase, containing water-insoluble binder for the fabrication of SCap electrodes. However, the drying procedure resulted in particle agglomeration, which hindered their mixing with NT. The major reasons of the agglomeration are the reduction of surface energy of MnO_2 nanoparticles and surface condensation reactions. In contrast, in this investigation we found that drying and re-dispersion steps can be avoided and MnO_2 particles can be prepared and mixed with NT in the *n*-butanol

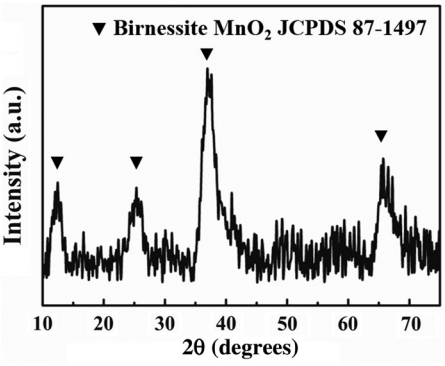


Figure 1. XRD pattern of MnO_2 powder.

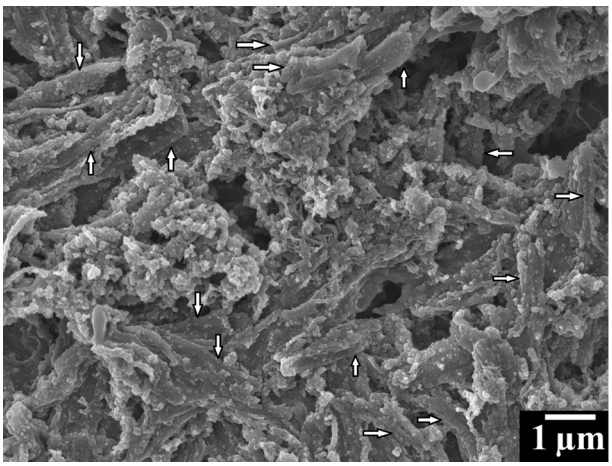


Figure 2. SEM image of MnO_2–NT composite; arrows show examples of elongated particles.

https://doi.org/10.1557/mrc.2018.165 Published online by Cambridge University Press

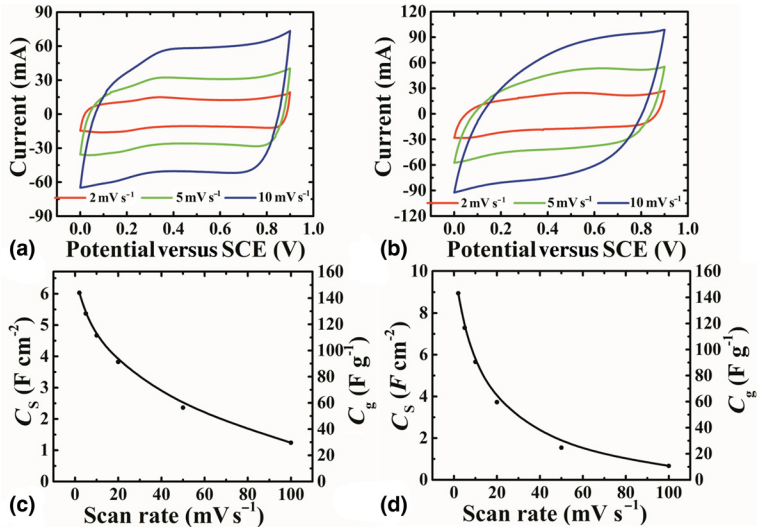


Figure 3. (a, b) CVs at different scan rates and (c, d) C_g and C_S versus scan rate for MnO_2–NT electrodes with AM of (a, c) 42 mg/cm^2 and (b, d) 61 mg/cm^2.

phase. As mentioned above, NTs can be transferred from water to *n*-butanol spontaneously without the use of a surfactant. However, the use of CPC facilitated dispersion of NTs and their transfer to *n*-butanol.

The addition of *n*-butanol to the aqueous phase, containing cetylpyridinium permanganate and NT led to the formation of a suspension of MnO_2 and NT (Supplementary Fig. S2). We suggest that CPC facilitated co-dispersion MnO_2 and NT as well as and their mixing. Moreover, we found that good dispersion facilitated the impregnation of Ni foam current collectors and allowed the fabrication of electrodes with high AM.

Figure 2 shows an SEM image of a MnO_2–NT composite formed by filtering and drying of the suspension of MnO_2 and NT in *n*-butanol. The SEM studies indicated that phase segregation of MnO_2 and NT was avoided. The microstructure showed many elongated particles, the formation of such particles is probably governed by the shape of NT encapsulated in the MnO_2 matrix. The SEM images at higher magnifications and transmission electron microscopy images revealed many MnO_2 coated NTs (Supplementary Figs. S3 and S4). The analysis of the electron microscopy data showed improved mixing of MnO_2 and NT. As a result, we achieved improved electrode performance at high AM.

The capacitive performance of the electrodes was analyzed by different methods (Figs. 3 and 4, Supplementary Figs. S5–S7, Table S1). Figures 3(a) and 3(b), S5(a) show cyclic voltammetry (CVs) for MnO_2–NT composites with AM loadings in the range of 42–61 mg/cm^2. The nearly ideal box shape CVs represent good capacitive behavior, which was achieved at high AM. The capacitances of 6.03, 7.22, and 8.95 F/cm^2 were achieved for mass loadings of 42, 51, and 61 mg/cm^2, respectively, at a scan rate of 2 mV/s^1. However, C_S decreased with scan rate increase due to limited diffusion of electrolyte in pores [Figures 3(c) and 3(d), S5(b)]. The δ_m values were in the range of 0.63–0.91 for AM of 42–61 mg/cm^2. The relatively high δ_m values offer benefits for the fabrication of devices with reduced mass. The high capacitance was achieved at relatively low electrode resistance. Figures 4(a) and S5(c) show complex impedance data in the Nyquist diagram. For the

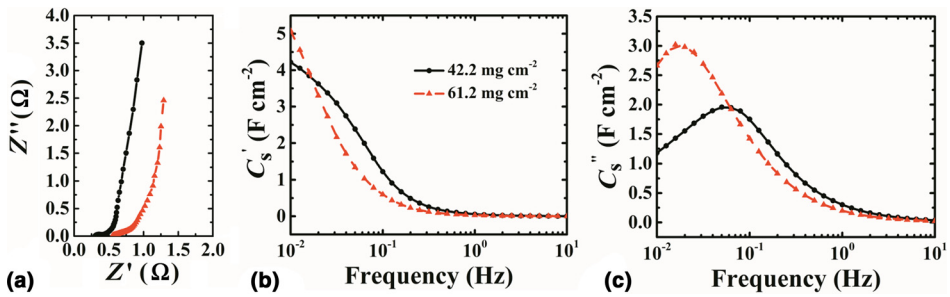


Figure 4. (a) Nyquist plots of complex impedance and (b, c) frequency dependences of components of complex capacitance for MnO_2–NT electrodes with AM of 42 and 61 mg/cm^2.

https://doi.org/10.1557/mrc.2018.165 Published online by Cambridge University Press

electrode with AM of 42 mg/cm^2 the slope of the graph was close to 90°, indicating good capacitive properties. The electrode with AM of 61 mg/cm^2 showed slightly higher resistance and reduced Nyquist diagram slope. The equivalent series resistance value increased from 0.97 to 1.27 Ohms with AM increase in the range of 42–61 mg/cm^2. The complex capacitance, derived from the AC impedance data [Figs. (4b) and 4 (c), S5(d)] showed a frequency dispersion of the relaxation type,[24,25] due to the decrease of the real part (C_S') with frequency increase and relaxation maxima in the imaginary part (C_S''). The frequency of the relaxation maximum decreased with increasing AM due to limited diffusion in pores. The constant current charge–discharge graphs (Supplementary Fig. S7) were of nearly ideal symmetric triangular shape, which indicated good capacitive properties.

Conclusions

A conceptually new method has been developed for the manufacturing of MnO_2–NT electrodes for SCaps. CPC was used as a complexing and capping agent for synthesis and a phase transfer agent for liquid–liquid particle extraction. We suggested a mechanism of synthesis, which involved the formation of cetylpyridinium permanganate in an aqueous phase, phase transfer to *n*-butanol phase and reduction of MnO_4^- species by *n*-butanol. In this method, the problem of particle agglomeration in the drying process was eliminated. The co-dispersion of MnO_2 and NT in *n*-butanol facilitated their improved mixing, which allowed the fabrication of advanced electrodes with high AM. We demonstrated the formation of SCap electrodes with AM loading in the range of 42–61 mg/cm^2. The high AM loading allowed for high δ_m, which was beneficial for the fabrication of SCap with reduced total mass. The electrodes showed enhanced capacitive behavior and low resistance. The highest C_S of 8.95 F/cm^2 was obtained.

Supplementary material

The supplementary material for this article can be found at https://doi.org/10.1557/mrc.2018.165.

Acknowledgment

This investigation was supported by NSERC Canada.

References

1. S. Devaraj and N. Munichandraiah: High capacitance of electrodeposited MnO_2 by the effect of a surface-active agent. *Electrochem. Solid-State Lett.* **8**, A373–A377 (2005).
2. T. Brousse, P.L. Taberna, O. Crosnier, R. Dugas, P. Guillemet, Y. Scudeller, Y Zhou, F. Favier, D. Belanger, and P. Simon: Long-term cycling behavior of asymmetric activated carbon/MnO_2 aqueous electrochemical supercapacitor. *J. Power Sources* **173**, 633–641 (2007).
3. Y.U. Jeong and A. Manthiram: Nanocrystalline manganese oxides for electrochemical capacitors with neutral electrolytes. *J. Electrochem. Soc.* **149**, A1419–A1422 (2002).
4. N.R. Chodankar, D.P. Dubal, G.S. Gund, and C.D. Lokhande: Bendable all-solid-state asymmetric supercapacitors based on MnO_2 and Fe_2O_3 thin films. *Energy Technol.* **3**, 625–631 (2015).
5. C.A. Beasley, M.B. Sassin, and J.W. Long: Extending electrochemical quartz crystal microbalance techniques to macroscale electrodes: insights on pseudocapacitance mechanisms in MnO_x-coated carbon nanofoams. *J. Electrochem. Soc.* **162**, A5060–A5064 (2015).
6. L. Athouël, P. Arcidiacono, C. Ramirez-Castro, O. Crosnier, C. Hamel, Y. Dandeville, P. Gillemet, Y. Scudeller, D. Guay, D. Belanger, and T. Brousse: Investigation of cavity microelectrode technique for electrochemical study with manganese dioxides. *Electrochim. Acta* **86**, 268–276 (2012).
7. L. Coustan, A. Le Comte, T. Brousse, and F. Favier: MnO_2 as ink material for the fabrication of supercapacitor electrodes. *Electrochim. Acta* **152**, 520–529 (2015).
8. L. Demarconnay, E. Raymundo-Pinero, and F. Béguin: Adjustment of electrodes potential window in an asymmetric carbon/MnO_2 supercapacitor. *J. Power Sources* **196**, 580–586 (2011).
9. Y. Lei, B. Daffos, P.L. Taberna, P. Simon, and F. Favier. MnO_2-coated Ni nanorods: enhanced high rate behavior in pseudo-capacitive supercapacitor. *Electrochim. Acta* **55**, 7454–7459 (2010).
10. F. Grote, R.S. Kühnel, A. Balducci, and Y. Lei: Template assisted fabrication of free-standing MnO_2 nanotube and nanowire arrays and their application in supercapacitors. *Appl. Phys. Lett.* **104**, 053904 (2014).
11. N. Goubard-Bretesché, O. Crosnier, G. Buvat, F. Favier, and T. Brousse: Electrochemical study of aqueous asymmetric $FeWO_4$/MnO_2 supercapacitor. *J. Power Sources* **326**, 695–701 (2016).
12. H. Xia and C. Huo: Electrochemical properties of MnO_2/CNT nanocomposite in neutral aqueous electrolyte as cathode material for asymmetric supercapacitors. *Int. J. Smart Nano Mater.* **2**, 283–291 (2011).
13. M. Borysiewicz, M. Wzorek, M. Ekielski, J. Kaczmarski, and T. Wojciechowski: Controlling the nanoscale morphology and structure of the ZnO/MnO_2 system for efficient transparent supercapacitors. *MRS Commun.* **7**, 173–178 (2017).
14. G.S. Gund, D.P. Dubal, N.R. Chodankar, J.Y. Cho, P. Gomez-Romero, C. Park, and C.D. Lokhande: Low-cost flexible supercapacitors with high-energy density based on nanostructured MnO_2 and Fe_2O_3 thin films directly fabricated onto stainless steel. *Sci. Rep.* **5**, 12454 (2015).
15. R. Chen, R. Poon, R.P. Sahu, I.K. Puri, and I. Zhitomirsky: MnO_2-carbon nanotube electrodes for supercapacitors with high active mass loadings. *J. Electrochem. Soc.* **164**, A1673–A1678 (2017).
16. S. Dash and B.K. Mishra: Mn(VII) oxidation using cetyltrimethylammonium permanganate: self-oxidation of CTAP and oxidation of benzyl alcohol. *Int. J. Chem. Kinet.* **27**, 627–635 (1995).
17. S. Uppugalla, R. Boddula, and P. Srinivasan: Methyl triphenylphosphonium permanganate as a novel oxidant for aniline to polyaniline-manganese(II, IV) oxide: material for high performance pseudocapacitor. *J. Solid State Electrochem.* **22**, 407–415 (2018).
18. S. Ching, E.J. Welch, S.M. Hughes, A.B. Bahadoor, and S.L. Suib: Nonaqueous sol-gel syntheses of microporous manganese oxides. *Chem. Mater.* **14**, 1292–1299 (2002).
19. S. Dash, S. Patel, and B.K. Mishra: Oxidation by permanganate: synthetic and mechanistic aspects. *Tetrahedron* **65**, 707–739 (2009).
20. H. Karaman, R.J. Barton, B.E. Robertson, and D.G. Lee: Preparation and properties of quaternary ammonium and phosphonium permanganates. *J. Org. Chem.* **49**, 4509–4516 (1984).
21. C. Wallar, T. Zhang, K. Shi, and I. Zhitomirsky: Synthesis of metal and metal oxide nanoparticles, liquid–liquid extraction and application in supercapacitors. *Colloids Surf., A* **500**, 195–202 (2016).
22. M.A. Malik and Z. Khan: Permanganate transfer and reduction by D-glucose in benzene-cetyltrimethylammoniumbromide aqueous solution: a kinetic study. *Int. J. Chem. Kinet.* **40**, 496–503 (2008).
23. Y. Wang, Y. Liu, and I. Zhitomirsky: Surface modification of MnO_2 and carbon nanotubes using organic dyes for nanotechnology of electrochemical supercapacitors. *J. Mater. Chem. A* **1**, 12519–12526 (2013).
24. K. Shi and I. Zhitomirsky: Influence of current collector on capacitive behavior and cycling stability of Tiron doped polypyrrole electrodes. *J. Power Sources* **240**, 42–49 (2013).
25. Y. Su and I. Zhitomirsky: Asymmetric electrochemical supercapacitor, based on polypyrrole coated carbon nanotube electrodes. *Appl. Energy* **153**, 48–55 (2015).

https://doi.org/10.1557/mrc.2018.165 Published online by Cambridge University Press